Contents lists available at ScienceDirect

Measurement

journal homepage: www.elsevier.com/locate/measurement

Intelligent fall detection method based on accelerometer data from a wrist-worn smart watch

Lin Chen [a], Rong Li [a], Hang Zhang [b], Lili Tian [b], Ning Chen [b]

[a] State Key Laboratory of Advanced Design and Manufacturing for Vehicle Body, Hunan University, Changsha 410082, PR China
[b] College of Mechanical and Vehicle Engineering, Hunan University, Changsha 410082, PR China

ARTICLE INFO

Article history:
Received 2 December 2018
Received in revised form 27 February 2019
Accepted 29 March 2019
Available online 11 April 2019

Keywords:
Fall detection
Wearable device
Stacked autoencoder
One-class classification based on the convex hull
Ensemble strategy

ABSTRACT

Accurate and reliable automatic fall detection based on wearable devices enables elderly people to receive instant treatment and can alleviate the severe consequences of falls. Falls are abnormal activities that occur rarely compared with normal daily activities; therefore, fall detection can be considered a one-class classification problem. However, it is difficult and dangerous to collect sufficient fall data in practice, making it difficult to use supervised learning methods to detect falls automatically. Among wearable devices, wrist-worn devices for fall detection are more likely to be accepted because of comfort; however, high accuracy cannot typically be realized due to sensitivity to interference from the diverse activities of the hand and wrist. Combining ensemble stacked autoencoders (ESAEs) with one-class classification based on the convex hull (OCCCH), this paper proposes a novel intelligent fall detection method, namely, ESAEs-OCCCH, which is based on accelerometer data from a wrist-worn smart watch. In the proposed method, ESAEs are first adopted for unsupervised feature extraction to overcome the disadvantages of artificial feature extraction, namely, the requirements in terms of experience and time. Then, OCCCH is used for pattern recognition. Finally, the majority voting strategy and weight adaptive adjustment strategy are combined to improve the performance and stability of fall detection. According to the behavioral characteristics of the elderly, the uncertainty of activities of daily living (ADLs) and fall activities (FAs), and the influence of the intense activities of the hand on the accelerometer signal, thirteen FAs and sixteen ADLs, including intense hand and wrist activities, are simulated by young volunteers of various genders, ages, heights and weights in two experiments. The experimental results demonstrate the performance and stability of the proposed method.

1. Introduction

With the percentage of the aging population who lives alone increasing constantly, fall incidents are becoming a major health care problem for elderly people in contemporary society. Falls are the leading cause of accidental injuries and deaths for the elderly people who are over 65 years old [1]. The annual incidence of falls in the elderly is approximately 35% and increases with age [2]. Falls may have serious consequences; however, most serious consequences are not directly caused by falls but by lack of timely assistance and treatment [3]. Sending an immediate alarm to the caregiver of an elderly person who has fallen can prevent further damage, reduce treatment costs and increase the opportunities for recovery. Hence, it is of substantial importance and necessity to develop an accurate, convenient and reliable automatic fall detection system.

In the past two decades, wearable-based systems have been widely adopted for fall detection due to their availability at any time and in any place [4,5]. Most wearable devices realize fall detection using motion sensors such as accelerometers, gyroscopes and magnetometers [6,7], which are placed on parts of the body, such as the head, waist, and wrist [8]. Threshold-based algorithms and intelligent algorithms are two main methods that are used in fall detection with wearable devices [9,10]. For threshold-based fall detection algorithms, the classification of fall and nonfall events is performed by artificially comparing and selecting the optimal threshold from statistical features of the motion dynamics; low computational complexity is its main advantage. However, fixed threshold-based techniques are not suitable for detecting various types of falls and cannot be applied to individuals who differ in height and weight. The other approach is intelligent detection algorithms [11,12], which have been increasingly used for fall detection in the past ten years. Traditional intelligent fall

https://doi.org/10.1016/j.measurement.2019.03.079

detection algorithms mainly consist of three steps: feature extraction, feature selection, and pattern recognition [13]. Effective feature extraction and feature selection often require practical experience, rich prior knowledge and substantial computing time. In addition, the fall sensor signals of the elderly are complicated, variable and dangerous to acquire; hence, it is highly difficult to ascertain the number or types of fall features. With the rapid development of deep learning in the past five years, which can automatically extract features [14], it has been gradually applied to fall detection with wearable devices [15,16].

Substantial investigation into the optimal locations for sensors has been performed for over ten years. By attaching triaxial accelerometers at the waist, wrist and head, Kangas et al. (2007) [17] investigated the recorded accelerometer signals to determine threshold values for multiple parameters for discriminating between fall activities (FAs) and activities of daily living (ADLs) and compared the resulting fall detection accuracies. The results demonstrate that the wrist-located accelerometer has lower fall detection accuracy than the accelerometers that are located on the waist and head and the accuracy is only 75%. Özdemir et al. (2016) [18] conducted fall detection research by using principal component analysis (PCA) to extract features. The sensors, including an accelerometer, gyroscope and magnetometer, were placed on various parts of the body: head, chest, waist, right wrist, right thigh, right ankle and chest. Six machine learning algorithms, namely, k-nearest neighbor (KNN), bayesian decision making (BDM), support vector machines (SVM), least squares method (LSM), and artificial neural networks (ANNs), were used as classifiers. The results demonstrate that wrist sensor performs the poorest in terms of accuracy. Gjoreski et al. (2016) [19] compared the performances of accelerometers that were positioned at various locations of the body based on four datasets [20]. The results demonstrate that accelerometers that are positioned at the wrist outperform those at the elbow and chest and accelerometers that are positioned at the ankle, knee and belt realize the best performance. The sensor on the left wrist realizes 72% accuracy and that on the right wrist realizes 68% accuracy on the JSI dataset and that on the right wrist realizes 76% accuracy on the Sports dataset. Based on the above studies, the fall detection accuracy of wrist-worn devices is much lower than those of devices on other body parts, regardless of whether threshold-based algorithms or intelligent algorithms are used.

However, the wrist-worn smart watch is one of the most comfortable devices among wearable devices, which can be worn conveniently by users [21,22]. Therefore, many scholars have conducted research on the fall detection based on wrist-worn devices. Zhou et al. (2014) [23] investigated forward fall detection via summing the vector thresholds of acceleration data and realized an accuracy of 93.75%. In the experimental design, ADLs include stationary scenarios, walking, and standing up from sitting. Yuan et al. (2015) [21] proposed a power-efficient interrupt-driven threshold-based algorithm for fall detection based on accelerometer data. Experimental results demonstrate that the wrists of experimenters occasionally hit the desk with high impact in the process of sitting down at a desk, which may accidentally trigger a false-positive fall alarm. Although 96.4% accuracy is realized, the ADLs only include walking, walking upstairs, walking downstairs, sitting down in a chair beside a desk and other activities such as writing, picking up and putting down random objects. In the above studies, the frequent random movements of the hand and wrist, especially the high impact motions in daily life, which may lead to misjudgments, are rarely included in the experimental design. Ngu et al. (2018) [24] conducted fall detection research by computing acceleration features over a sliding window. In addition to common ADLs such as jogging, sitting down, throwing an object and waving hands are included in the ADLs experiment and 93.33% accuracy is realized using a naive bayes machine learning model. Quadros et al. (2018) [25] conducted fall detection research for wrist-worn devices that were equipped with three sensors (accelerometer, gyroscope and magnetometer) and improved the classification of ADLs. In the experimental design, not only walking and sitting on a chair but also the frequent random movements of the hand and wrist, such as clapping hands, opening and closing a door, moving an object, and tying shoes, are considered as ADLs. The results demonstrate that the fall detection accuracy that was realized by the machine learning methods is considerably higher than that of threshold-based algorithms. Among the five machine learning methods (KNN, linear discriminant analysis (LDA), logistic regression (LR), decision tree (DT), and SVM), the best result of 99% accuracy is realized by the KNN method. According to the above studies, it is difficult to realize a fall detection accuracy of 95% with accelerometer data-based wrist-worn devices due to interference from the frequent random movements of the hand and wrist. Considering the cost and energy consumption of multiple sensors, this paper focuses on intelligent algorithms for fall detection that utilize accelerometer data from a wrist-worn smart watch. Based on the behavioral characteristics of the elderly and an analysis of the accelerometer data, intense hands activities are considered in experimental design. Moreover, all experiments are performed by young volunteers.

For realizing fall detection via intelligent algorithms, feature extraction and pattern recognition are essential. Falls are abnormal activities that occur rarely; hence, it is difficult to collect real FAs data, especially for elderly people. Even simulated fall experiments by young volunteers cannot fully cover all fall behaviors. Therefore, fall detection can be considered a one-class classification problem and it is difficult to use supervised learning methods to automatically detect falls. In comparison, the data of ADLs are easy to collect. The data imbalance between ADLs and FAs could lead to the failure of traditional binary classification methods. During the last ten years, several one-class classification methods were used in fall detection [26]; among them, one-class support vector machine (OCSVM) is a popular approach for fall detection and exhibits effective classification performance [27]. Aiming at overcoming the inefficiency of OCSVM, Zeng et al. (2016) [28] proposed one-class classification based on the convex hull (OCCCH) and applied it to the fault detection of roller bearing. Experimental results demonstrate that OCCCH with the generalized gilbert algorithm is more efficient than OCSVM with the well-known sequential minimal optimization (SMO) algorithm and OCCCH can realize comparable classification accuracy to OCSVM. Considering the efficiency of the fall detection algorithm, this paper utilizes OCCCH as the classifier.

Since supervised learning methods are not suitable for fall detection and the rapid development of deep learning in the past five years has made unsupervised feature extraction possible, deep learning is adopted for unsupervised feature extraction in this paper. In contrast to deep belief networks (DBN) and convolutional neural networks (CNN), an autoencoder (AE) is a purely unsupervised feature learning model that has powerful feature extraction capabilities and excellent learning performance and it has been widely applied in various fields, such as computer vision [29], image classification [30], and rolling bearing fault diagnosis [31]. However, due to the simplicity of the individual network structure, the individual AE model exhibits low generalization performance on diverse, massive and complex data. The ensemble strategy is one of the effective strategies for reducing model variance and improving model generalization performance [32]. Currently, unsupervised learning methods are rarely applied to fall feature extraction with wearable devices. Khan et al. (2017) [26] proposed ensemble autoencoders (EAEs) for learning features from channels of wearable sensor data. The one-class nearest neighbor approach (OCNN) and OCSVM are used as classifiers; however, the resulting geometric means (gmeans) do not exceed 50%. By designing a series of AEs with various characteristic activation functions, Shao et al. (2018) [32] proposed a novel method, namely, ensemble deep AEs (EDAEs), for fault diagnosis of rolling bearings. Experiment results demonstrate that the testing accuracy of EDAEs is 97.18%, which is 3.1% higher than the highest accuracy among the fifteen individual DAEs. Therefore, to improve the performance and stability of the individual AE model, ensemble stacked autoencoders (ESAEs) are utilized in this paper to perform unsupervised feature extraction and a novel fall detection method, namely, ESAEs-OCCCH, is proposed that utilizes accelerometer data from a wrist-worn smart watch, in which ESAEs are used to extract signal features and OCCCH is utilized for pattern recognition.

The remainder of this paper is organized as follows: Section 2 describes the proposed method in detail. Section 3 presents the experimental work, including the wrist-worn smart watch, signal preprocessing, activity classification, experiments and volunteers, and evaluation indices. Section 4 presents the experimental evaluations, compares the results and analyzes the implementability of the proposed method. Section 5 presents the conclusions of our work.

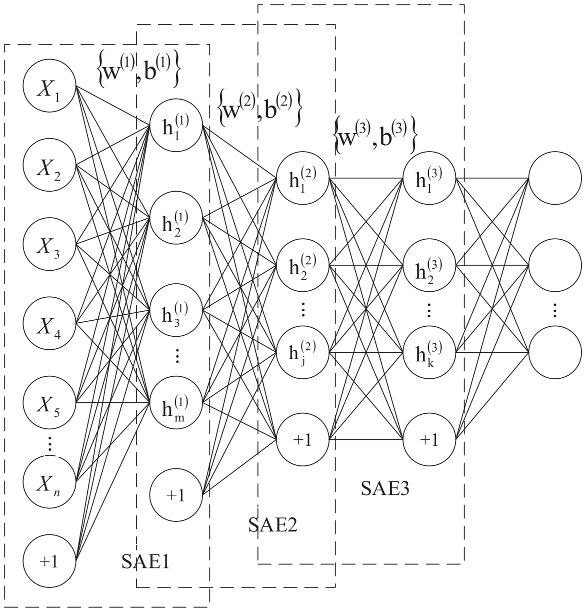

Fig. 1. Structure of the SAEs network.

2. ESAEs-OCCCH method

2.1. Brief introduction to stacked autoencoders (SAEs)

An AE is a typical unsupervised feature learning approach, which can automatically learn features from unlabeled data. The main strategy of AE is to minimize the reconstruction error so that its outputs are similar to its inputs. An AE is a three-layer symmetric neural network, which includes an input layer, a hidden layer and an output layer.

An AE includes an encoder and a decoder. The encoder, which consists of an input layer and a hidden layer, maps the input data from a high-dimensional feature vector onto a low-dimensional hidden feature vector. Consider a training sample, namely, $x = \{x^{(1)}, x^{(2)}, \ldots, x^{(D)}\}$, where $x \in R^{D\times 1}$ is the input layer and has D-dimensional features of the original data. Via a linear mapping and nonlinear activation function $h = f(W_1 x + b_1)$, x is encoded into a d-dimensional hidden layer: $h = \left[h^{(1)}, h^{(2)}, \ldots, h^{(d)}\right]$, where $h \in R^{d\times 1}$, $W_1 \in R^{d\times D}$ is a weight matrix of the encoder, $b_1 \in R^{d\times 1}$ is a bias term of the encoder, and f is an activation function. Similarly, the hidden layer and output layer constitute a decoder, which maps the hidden feature vector, namely, h back to a reconstruction feature vector, namely, $z = \left[z^1, z^2, \ldots, z^D\right]$, and $z \in R^{D\times 1}$. Set $z = f(W_2 h + b_2)$, where $W_2 \in R^{D\times \mathrm{d}}$ is a weight matrix of the decoder and $b_2 \in R^{D\times 1}$ is a bias term of the decoder.

Defining the parameter set $\theta = (W_1, b_1, W_2, b_2)$, the objective of the AE training is to minimize the reconstruction error by optimizing θ. Given a set of fixed training sets with m training examples, we define the minimized reconstruction error function, which is denoted as $J(\theta)$, as follows:

$$J(\theta) = \sum_{i=1}^{m} \frac{1}{2} \| z_i - x_i \|^2 \tag{1}$$

The SAEs is constructed with several AEs, as illustrated in Fig. 1; in the example, the SAEs consists of SAE1, SAE2 and SAE3. Although SAEs can be used for unsupervised feature extraction in fall detection, individual SAEs have low generalization ability [32].

2.2. Brief introduction to OCCCH

The basic strategy of OCCCH is to determine the nearest point to the origin from the convex hull of training samples; then, the separating hyper-plane is completely determined by the nearest point. Any point that lies on the separating hyper-plane satisfies $\langle w, x\rangle - b = 0$, where w and b are the normal and the bias, respectively. Assume $X = \{x_i\}_{i=1}^{l}$ are training samples whose labels are all negative. In the linearly inseparable case, the problem of finding the nearest point from the reduced convex hull to the origin can be formulated as the following nearest-point problem:

$$\begin{aligned} &\min_{\alpha\in R} \| \sum_{i=1}^{l} \alpha_i x_i \| \\ &s.t. \quad \sum_{i=1}^{l} \alpha_i = 1, 0 \le \alpha_i \le \mu, i = 1, 2, \ldots, l \end{aligned} \tag{2}$$

where α_i are the combination coefficients and $\mu \in [1/l, 1)$ is the reduction factor.

Given the optimal solution, which is denoted as $\alpha^* = \left(\alpha_1^*, \alpha_2^*, \ldots, \alpha_l^*\right)^T$ and denoting by x^* the corresponding nearest point, $w^* = x^* = \sum_{i=1}^{l} \alpha_i^* x_i$ and $b^* = \langle w^*, x^*\rangle$ can be computed, where b^* is the inner product of w^* and x^*. The points on the separating hyper-plane satisfy $\langle w^*, x\rangle - b^* = 0$. Thus, the classification of an unknown sample can be determined via a decision function: $f(x) = \langle w^*, x\rangle - b^*$. If $f(x) \ge 0$, then x is accepted into the target class; otherwise, it is rejected from the target class and accepted into the nontarget class. The basic strategy of OCCCH is illustrated in Fig. 2. As discussed in the introduction, fall detection can be considered a one-class classification problem, in which ADLs samples can viewed as the target class, and OCCCH is more efficient than OCSVM [28]. Thus, OCCCH is used for pattern recognition for fall detection in this paper.

2.3. Proposal of ESAEs-OCCCH

ESAEs overcome the limitations of individual SAEs and enhance the generalization performance. To realize higher classification

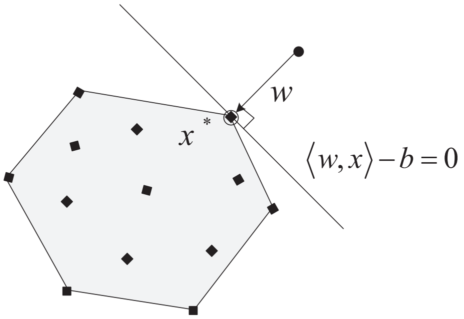

Fig. 2. Illustration of the basic strategy of OCCCH.

performance for ensemble learning, it is necessary to consider ensemble diversity. Ensemble diversity refers to the difference among individual learners. To realize model diversity, various numbers of hidden layers and their hidden nodes in the SAEs architectures and activation functions of the SAEs can be utilized. Wang et al. (2017) [33] proposed EAEs with various numbers of hidden layers, as feature layers differ in terms of identification ability, and the experimental results demonstrate the performance of the method for induction motor fault diagnosis. To overcome the limitations of individual deep learning models, Shao et al. (2018) [32] proposed EDAEs with various characteristic activation functions via an adaptive weight adjustment strategy and applied them successfully to fault diagnosis for rolling bearings. Inspired by these works, a new ESAEs method that differs in terms of SAEs architectures and activation functions is proposed for fall detection in this paper.

Considering the efficiency, we select four commonly used activation functions: the sigmoid, rectified linear unit (Relu), softplus, and gaussian functions. As the SAEs architectures affect the accuracy and efficiency of pattern recognition, three types of SAEs architectures are proposed, which are designed via many trials; the process is described in detail in Section 4.1. Among the ensemble strategies, the majority voting strategy and weight adaptive adjustment strategy have frequently been utilized in the recent literature in many fields [34]. To reduce the impact of the SAEs architectures on the fall detection results under the same activation function, we use the majority voting strategy to realize the first ensemble and the weight adaptive adjustment strategy to realize the second ensemble according to the sensitivity under four activation functions. Through two steps of ensembles, ESAEs-OCCCH is constructed for overcoming the limitations of the individual SAEs and enhancing the generalization performance.

2.4. Procedure of ESAEs-OCCCH

Accelerometer data of ADLs and FAs are collected by an accelerometer in two simulated experiments with different groups of young volunteers. The experimental work is discussed in Section 3, including the device, signal preprocessing, activity classification, experiments, volunteers and evaluation indices. All training samples are from ADLs and the testing samples are from ADLs and FAs. Then, ESAEs-OCCCH is constructed from two ensembles. The training samples are divided into two parts: a set of most of the training samples, which is called training samples I, are used for the construction of the twelve SAEs-OCCCHs, as illustrated in Step 1; the set of the remaining samples, which is called training samples II, are used to calculate the weight of the second ensemble, as expressed in Eq. (4) of Step 3.

The framework of the proposed method, namely, ESAEs-OCCCH, for fall detection of elderly people, is illustrated in Fig. 3 and the procedures are summarized as follows:

For activation functions = {Sigmoid, Relu, Softplus, Gaussian}:

Step 1: Model training of twelve SAEs-OCCCHs

First, training samples I are used to train twelve SAEs-OCCCHs. Then, the corresponding prediction results, which are denoted as pr_m, are calculated, where $m = (1,2,3)$, $m = (4,5,6)$, $m = (7,8,9)$, and $m = (10,11,12)$ represent three SAE architectures under the sigmoid, relu, softplus, and gaussian activation functions, respectively.

Step 2: Majority voting ensemble

According to the majority voting strategy, the prediction results, namely, pr_i^1, under the same activation functions are calculated in the first ensemble and four ESAEs-OCCCH$_\text{i}$ models that are based on four activation functions are constructed accordingly. The prediction results are matrices that consist of 0 s and 1 s, which represent ADLs and FAs, respectively.

$$pr_i^1 = sign\left(\sum_{m=3i\ -\ 2}^{m=3i} pr_m\right) \tag{3}$$

where $i = (1,2,3,4)$ represents the four activation functions.

Step 3: Calculate the weights in the second ensemble

Based on pr_i^1, the sensitivity, which is denoted as Sen_i, under the four activation functions can be obtained from training samples II. Define a threshold β such that only if $\text{Sen}_\text{i} \geq \beta$ does ESAEs-OCCCH$_\text{i}$ participate in the second ensemble. The higher Sen_i is, the larger the weight that is assigned to ESAEs-OCCCH$_\text{i}$. Thus, the weights of ESAEs-OCCCH$_\text{i}$ under the four activation functions are as follows:

$$weight_i = \frac{Sen_i - \beta}{\sum_{i=1}^{4} Sen_i - \beta} \tag{4}$$

with

$$Sen_i = \begin{cases} 0, & Sen_i \ \leq \beta \\ Sen_i, & Sen_i \ > \beta \end{cases} \tag{5}$$

The final prediction results, which are denoted as pr^2, are obtained via the weight ensemble strategy and the sign function that is specified below; then, ESAEs-OCCCH is finally constructed.

$$pr^2 = sign(\sum_{i=1}^{4} weight_i * pr_i^1) \tag{6}$$

3. Experimental work

3.1. Wrist-worn smart watch

In this work, an intelligent method for fall detection is proposed that is based on data from a commercial smart watch, which has 4 GigaByte physical memory and is equipped with a BM160 sensor. The sensor contains a triaxial accelerometer with a range of ±8 g. The triaxial accelerometer captures body accelerometer signals as a three-dimensional vector, which contain x-, y- and z-axis components AX, AY and AZ, respectively. The x-, y- and z-axis capture the horizontal movement, the forward movement, and the upward motion of the smart watch, respectively. The sampling frequency of the sensor is set to 220 Hz, which exceeds the frequency of human activities. The current consumption is 925 microampere. The construction and updating of the intelligent model for fall detection will be completed in the background server system; only the testing will be executed on the smart watch.

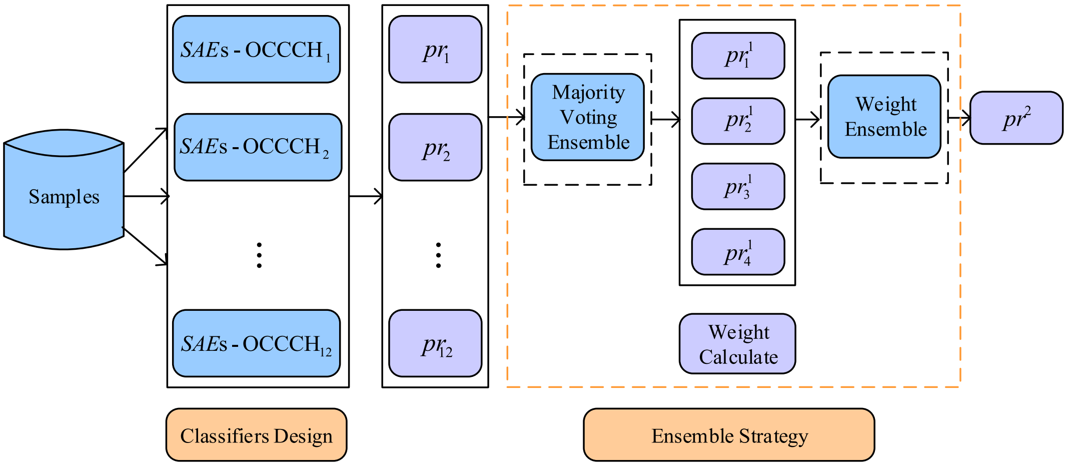

Fig. 3. Structure of ESAEs-OCCCH.

3.2. Signal preprocessing

After signal acquisition, each accelerometer signal is processed by a sliding window, where each window represents a sample. To ensure fall monitoring of the users, it is necessary to set the window overlap rate. Considering previous research work and the efficiency and accuracy of the fall detection system, the fixed-size overlapping sliding window (FOSW) overlap is set to 50% [35]. Fig. 4 shows an example of a four-second fall accelerometer signal. The sliding window size is two seconds and there are three sliding windows, as shown in the figure. Then, the collected samples are saved for subsequent analysis after signal processing with the sliding window.

3.3. Activity classification

In the simulated experiments, the activities of the young volunteers are divided into two categories: FAs and ADLs. Based on past research work [36,37], three main factors are considered in the experimental design: the behavioral characteristics of the elderly, the uncertainty of ADLs and FAs, and the influence of the intense activities of the hand on the accelerometer signal. Thirteen FAs and sixteen ADLs are designed in the experiments.

The FAs are classified according to the cause and direction of the fall. According to the cause of the fall, the FAs are divided into slipping, stepping on the air, tripping, knocking down, and sitting down on the ground. The FAs in the first three categories can be further divided into three subcategories according to the direction, namely, forward fall, backward fall, and sideways fall, as shown in Fig. 5. Sitting down on the ground only includes backward fall. According to the signals decomposition of the FAs, as illustrated in Fig. 6(a–c), the measured fall accelerometer signals of FAs of the same type that are performed by different volunteers are similar and strong impacts are observed in AX, AY, and AZ. In addition, the measured fall accelerometer signals of FAs of different types that are performed by the same volunteer have similar characteristics, as shown in Fig. 6(d–f).

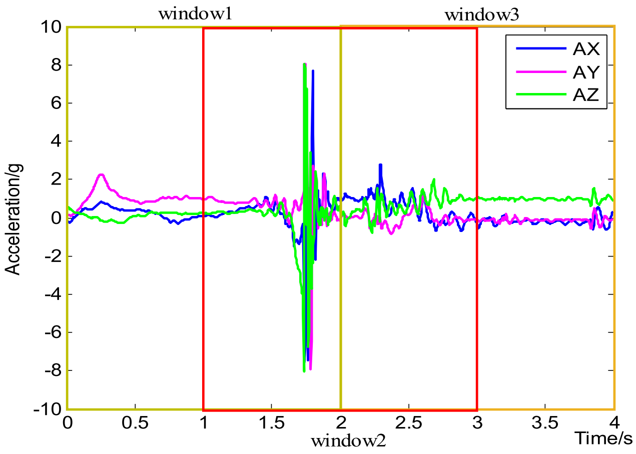

Fig. 4. Example of a fall accelerometer signal with a sliding window.

In view of the behavioral characteristics of the elderly, the ADLs include sedentary, walking, running, lying down, bending over, eating, walking upstairs, walking downstairs, going up by elevator, going down by elevator, quickly sitting down, and quickly standing up. Meanwhile, considering the intense activities of the hand that are likely to generate false alarms, four similar ADLs are included based on an analysis of the accelerometer data: applause, knocking on the table, waving and exercise. The four ADLs easily generate impact accelerometer signals. Knocking on the table and applause involve sudden stops of hand and wrist actions and the impacts between palms or between a palm and the table, which may trigger accelerometer signals in a smart watch. As knocking on the door and hammering nails are of the same ADL type as knocking on the table, they are considered to constitute a category. Waving is defined as waving the hands between left and right repeatedly, and exercise includes random movements of hands and arms, dancing activities, and daily exercise of the elderly, such as sword fighting, tai chi, and square dancing. Compared with applause and knocking on the table, the movements in waving and exercise are more random and involve sudden and quick activities of the hands.

To investigate how these intense movements of the hands and wrists of ADLs affect the accelerometer signal and evaluate the rationality of the ADLs classification, four accelerometer signals, namely, knocking on the table, applause, waving and exercise, are analyzed, as shown in Fig. 7(a–d). Running and quickly sitting down are selected as activities for comparison, as shown in Fig. 7(e–f). Both knocking on the table and applause generate much stronger instantaneous impacts in AZ, AY, or AX than the other four ADLs, which have similar characteristics to the FAs in Fig. 6. Although waving has an impact at the moment the hands stop, exercise in a random direction and running, which involve horizontal movements of the hands, are accelerated, the impacts are weaker and periodic. Quickly sitting down has a negligible impact. The figures for other ADLs are omitted due to space limitations. Based on the above analyses, sixteen ADLs and thirteen FAs are

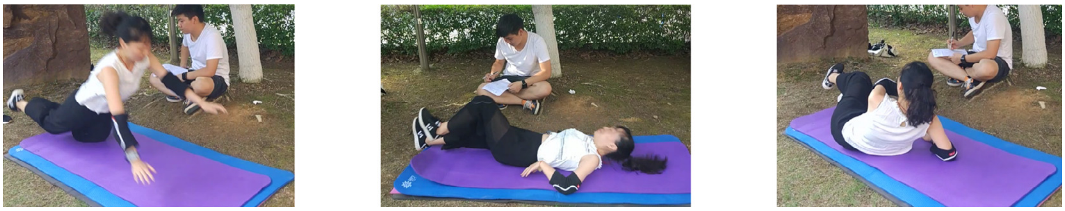

(a) Forward fall (b) Backward fall (c) Sideways fall

Fig. 5. Three directions of FAs.

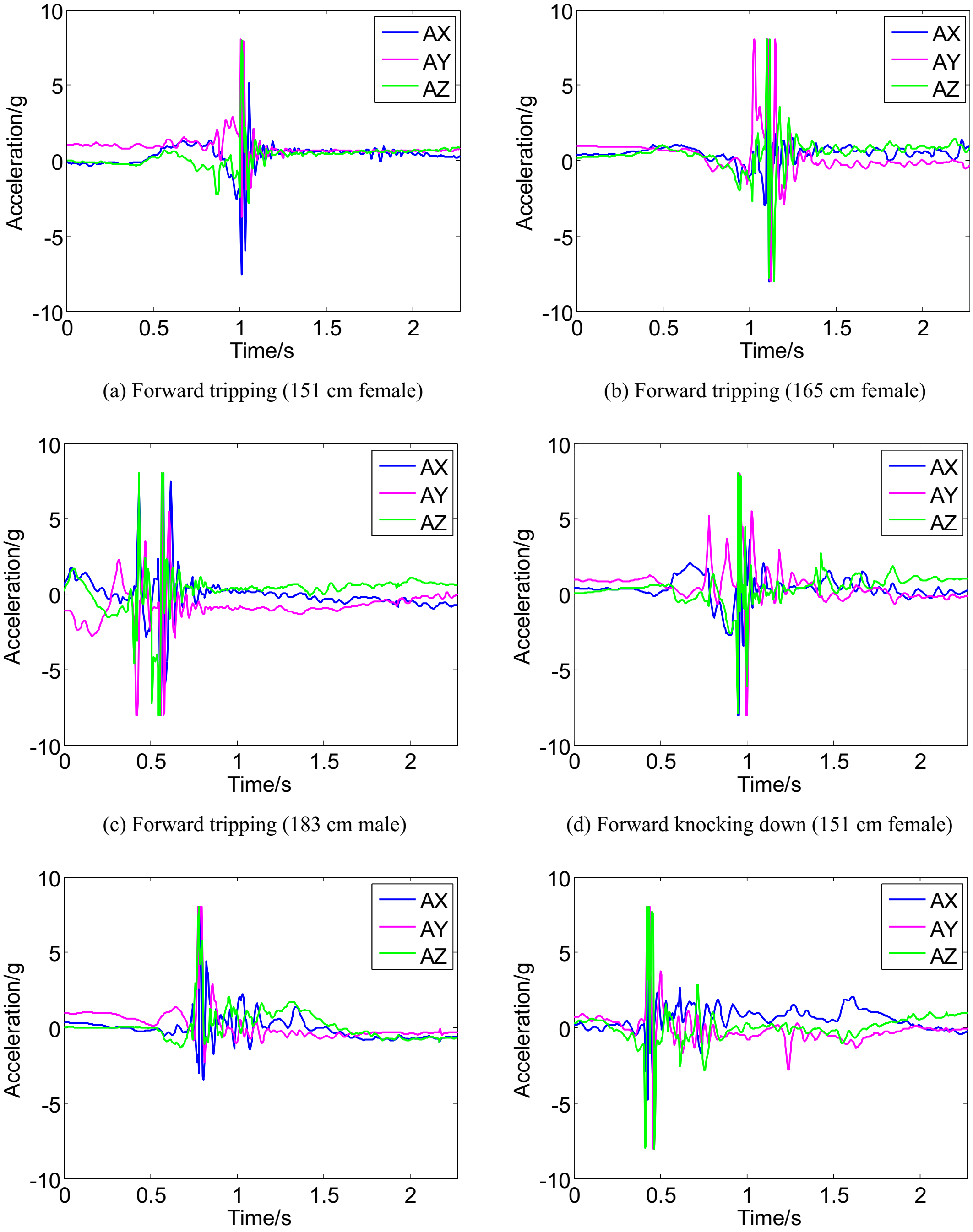

(a) Forward tripping (151 cm female)

(b) Forward tripping (165 cm female)

(c) Forward tripping (183 cm male)

(d) Forward knocking down (151 cm female)

(e) Backward knocking down (151 cm female)

(f) Sideways knocking down (151 cm female)

Fig. 6. Six accelerometer signals of three volunteers and three directions of FAs.

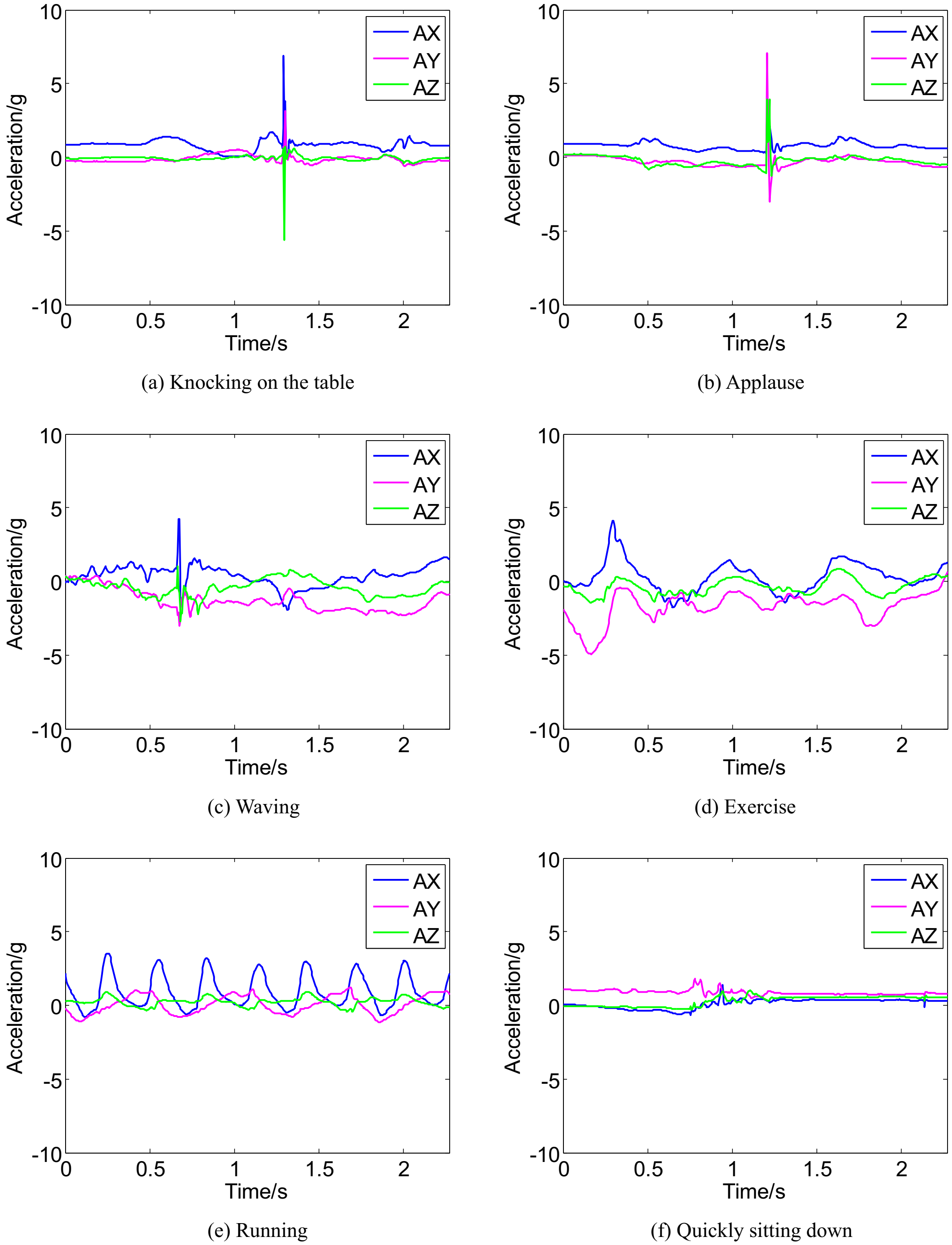

(a) Knocking on the table

(b) Applause

(c) Waving

(d) Exercise

(e) Running

(f) Quickly sitting down

Fig. 7. Six accelerometer signals that correspond to knocking on the table, applause, waving, exercise, running and quickly sitting down.

selected, which are listed in Table 1, and they are performed by young volunteers in simulated experiments, as described in Section 3.4.

3.4. Experiments and volunteers

In the model establishment and verification stage, the experiments are set up. As it is harmful and unsafe for the elderly to simulate FAs and ADLs, all the subjects are healthy young volunteers. As discussed in Section 3.3, the fall detection result from a smart watch is uncertain due to its sensitivity to interference from all kinds of activities of the hand and wrist and the uncertainty of ADLs and FAs in the experimental design. Considering the uncertainty of the proposed method, two experiments with different groups of volunteers are designed, which are referred to as experiment I and extended experiment II. Six volunteers of various genders, ages, heights and weights perform ADLs and FAs in experiment I; details about volunteers are listed in Table 2. In these experiments, all ADLs and FAs are repeated three times and the experimental order is random. All FAs experiments are performed on an outdoor yoga mat with a thickness of 2.4 cm and the ADLs experiments are performed in both indoor and outdoor environments. There are 288 ADLs and 234 FAs experiments in total.

Table 1
FAs and ADLs that are designed in the experiment I.

Activities		
FAs	backward fall	slipping, stepping on the air, tripping, knocking down, and sitting down on the ground
	forward fall	slipping, stepping on the air, tripping, and knocking down
	sideways fall	slipping, stepping on the air, tripping, and knocking down
ADLs	sedentary, walking, running, lying down, bending over, eating, walking upstairs, walking downstairs, going up by elevator, going down by elevator, quickly sitting down, quickly standing up, knocking on the table, waving (between left and right repeatedly), exercise (moving the hands and arms with random direction), and applause	

In extended experiment II, eleven volunteers perform the ADLs continuously and freely outdoors and the collected data correspond to real daily activities. All FAs are repeated five additional times randomly. The heights, genders, weights and ages of the eleven volunteers are listed in Table 3. All ADLs and FAs in the two experiments are performed randomly in terms of the magnitude and direction of motion.

Based on video recordings of all fall experiments, the length of each fall accelerometer signal is measured. The results demonstrate that a completed fall action contains preimpacts, impacts, and postimpacts and is completed in approximately 2 s on average. Thus, each fall sample is set to 500 data points, which is equivalent to 2.3 s. In experiment I, one hundred windows of each ADL and one window of each FA are collected; hence, a total of 28,800 ADLs samples and 234 FAs samples are processed. Many more ADLs samples are processed than FAs samples. In extended experiment II, the testing samples include 2000 ADLs samples and 55 FAs samples. All data processing is performed in MATLAB (R2014a, The Math Works, Inc.).

3.5. Evaluation indices

In the experimental evaluation, three indicators, namely, sensitivity, specificity and gmean [26], are typically used to assess the classification performance of fall detection based on an unbalanced dataset. Sensitivity refers to the percentage of nonfall events that are correctly classified and specificity refers to the percentage of fall events that are correctly classified. Due to the imbalance of the experimental data, the accuracy index is not suitable here; hence, we use gmean to represent the comprehensive accuracy of fall detection. The three indicators are expressed as follows:

$$\text{sensitivity} = \frac{TP}{TP + FN} * 100\% \tag{7}$$

$$\text{specificity} = \frac{TN}{TN + FP} 0\, 100\% \tag{8}$$

$$\text{gmean} = \sqrt{\frac{TP}{TP + FN} \times \frac{TN}{TN + FP}} * 100\% \tag{9}$$

where true positive (TP) represents the number of samples that are correctly identified as ADLs, false negative (FN) represents the number of ADLs samples that are falsely identified as FAs, true negative (TN) represents the number of samples that are correctly identified as FAs, and false positive (FP) represents the number of FAs samples that are falsely identified as ADLs.

4. Experimental results and analysis

To evaluate the performance, stability and implementability of ESAEs-OCCCH, a series of comparisons are performed that involve unsupervised feature extraction and pattern recognition; the comparison process is described in detail as follows:

Step 1: ESAEs-OCCCH is compared with twelve SAEs-OCCCHs in terms of the performance and stability of the ESAEs in Section 4.1.

Step 2: To evaluate the unsupervised feature extraction performance of the ESAEs, ESAEs-OCCCH is compared with OCCCH with statistical features and OCCCH with statistical features is compared with OCSVM, SVM and KNN with statistical features to evaluate the pattern recognition performance of OCCCH, as discussed in Section 4.2.

Step 3: ESAEs-OCCCH is compared with twelve SAEs-OCCCHs and four methods (OCCCH, OCSVM, SVM, and KNN with statistical features) in terms of efficiency and the implementability of the proposed method is discussed in Section 4.3.

Step 4: The results of extended experiment II are analyzed, as discussed in Section 4.4.

4.1. Comparison with twelve SAEs-OCCCHs

To evaluate the performance and stability of the proposed method, the SAE structure is optimized based on training samples and ESAEs-OCCCH is compared with twelve SAE-OCCCHs.

To decrease the impact of randomness, the SAEs architecture optimization experiments are repeated three times and all comparative experiments are repeated ten times. In each trial, 288,000 ADLs samples are randomly divided into three subsets, with 19,200 samples in subset training samples I, 2000 samples in subset training samples II, and 7600 samples in subset testing samples. All 234 FAs samples are utilized as testing samples. Thus, there are 21,200 training samples and 7834 testing samples in total. Considering the efficiency and accuracy of the SAEs, the number of hidden layers is set to four, the number of hidden layer nodes does not exceed 40, and the numbers of nodes in the four hidden layers are denoted as n1, n2, n3, and n4.

First, n1 = [10 20 30 40] is utilized when the activation function is sigmoid. The experiments are conducted three times and the gmean averages are 95.80%, 95.70%, 94.41%, and 89.74%, respectively. The highest gmean average of training samples I is 95.80%; hence, n1 is set to 10. After the selection of n1, we set n2 = [20 30 40]. The gmean averages are 96.49%, 96.26%, and 96.04%, respectively; thus, n2 is set to 20. Similarly, n3 = 30 and n4 = 20 are obtained. Among them, the highest gmeans of the four hidden layers are 95.80%, 96.49%, 95.38% and 95.54%, respectively. Taking the performance and efficiency into account, we select the

Table 2
Details about the volunteers who perform FAs and ADLs in experiment I.

Number	1	2	3	4	5	6
height (cm)	165	174	183	151	158	165
gender	male	male	male	female	female	female
weight (kg)	52	74	80	46	51	53
age	24	23	24	25	25	25

Table 3
Details about the volunteers who perform FAs and ADLs in extended experiment II.

Number	1	2	3	4	5	6	7	8	9	10	11
height (cm)	169	170	174	172	173	174	175	181	185	163	164
gender	male	male	male	male	male	male	male	male	male	female	female
weight (kg)	52	51	70	74	76	79	62	75	81	47	46
age	26	25	43	25	24	24	28	25	28	24	27

Table 4
ESAEs with four activation functions and three SAEs architectures.

activation function	SAEs architecture
Sigmoid	1500-10, 1500-10-20,1500-10-20-30
Relu	1500-10, 1500-10-20,1500-10-20-30
Softplus	1500-10, 1500-10-20,1500-10-20-30
Gaussian	1500-20, 1500-20-30,1500-20-30-10

Table 5
Parameters of ESAEs-OCCCH.

	Description	Value
ESAEs	Number of SAEs	12
	Number of activation functions	4
	Number of hidden layers	3
	Mean activation	0.1
	Weight decay parameter	0.003
	Weight of the sparsity penalty	3
	Threshold β of the accepted accuracy	0.9
	Number of repeated trials	10
OCCCH	Kernel function parameter	RBF kernel
	Kernel parameter σ	2
	Reduction factor μ	1

first three hidden layers; thus, the architecture of the three-layer SAEs with the sigmoid activation function is set to 1500–10-20–30. In the same way, the architectures of SAEs with the other three activation functions are obtained, which are listed in Table 4.

Based on the optimized SAE structure, ESAEs-OCCCH is compared with twelve SAEs-OCCCHs. The parameter values of ESAEs-OCCCH are listed in Table 5. The weights of the four activation functions are acquired through ten trials and are listed in Table 6. The means and standard deviations of the specificity, sensitivity, and gmean for both ESAEs-OCCCH and the twelve SAEs-OCCCHs are compared and listed in Table 7.

According to Table 7, the mean specificities of the twelve SAEs-OCCCHs range from 85.33% to 99.50%, the mean sensitivities range from 87.84% to 95.58%, and the mean gmeans are between 89.95% and 96.73%. The highest specificity is realized by the two-hidden-layer SAEs-OCCCH with the sigmoid activation function, while the highest sensitivity and gmean are realized by the three-hidden-layer SAEs-OCCCH with the Softplus activation function. The specificity, sensitivity, and gmean of the proposed method reach 98.92%, 96.09%, and 97.45% respectively. Although among the twelve SAEs-OCCCHs, the specificities of six SAEs-OCCCHs are slightly higher than that of the proposed method, the proposed method outperforms all twelve SAEs-OCCCHs in terms of the sensitivity and gmean. The standard deviation of the gmean of the proposed method is 0.0011, which is the smallest. The stability of the method is higher when the standard deviation of the gmean is smaller. Therefore, the results of the above comparisons with the twelve SAEs-OCCCHs demonstrate the high performance and stability of ESAEs-OCCCH.

To evaluate the performance of the proposed method and identify the easily misjudged activities, the average sensitivities of the sixteen ADLs and the average specificities of the five FAs are listed in Figs. 8 and 9. According to Fig. 8, the sensitivities of seven ADLs, namely, sedentary, walking, lying down, eating, walking upstairs, going up by elevator and going down by elevator, can reach 100%. Among the four intense and frequent activities of hand and wrist that were intentionally designed in the ADLs experiments, waving and exercise can reach sensitivities of 90.97% and 95.20%, whereas applause and knocking on the table have lower sensitivities of only 50.3% and 70.2%. The fall detection results of the four ADLs accord with the accelerometer signal analysis in Fig. 7 of Section 3.3. According to Fig. 9, among FAs, sitting down on the ground has the lowest specificity of 83.33% (15/18); the specificities of the other FAs reach 100%. The Z-axis accelerometer signal of the smart watch is occasionally relatively weak while sitting down on the ground, as the wrists of the experimenters do not hit the ground with high impact, which may accidentally trigger a false-positive fall alarm, such as in fainting onto the couch or the ground.

4.2. Comparison with other classifiers

As binary classifiers, SVM and KNN have been used for fall detection recently and realize high accuracy [26]. Therefore, to improve the unsupervised feature extraction performance of ESAEs and the accuracy of OCCCH pattern recognition, four pattern recognition methods with statistical features, namely, OCSVM, SVM, KNN and OCCCH, are compared with ESAEs-OCCCH.

According to the research work of Gjoreski et al. (2016) [19] and our research work, thirty statistical features that are widely used for fall detection are selected and listed in Table 8, including twenty-four time-domain statistical parameters and six frequency-domain statistical parameters. These features provide information about body posture (Mean X/Y/Z, Total mean, and Absolute area X/Y/Z), motion shape (Skewness X/Y/Z, Kurtosis X/Y/Z), motion variation (Variance X/Y/Z), and motion frequency (Mean X/Y/Z in the frequency domain and Standard Deviation X/Y/Z in the frequency domain).

Since the binary-class methods are utilized in this section, two-thirds of the FAs samples are used for training and one-third are used for testing; the ADLs samples that are used for testing and training are the same as in Section 4.1. Therefore, for SVM and KNN, 19,356 training samples, which consist of 19,200 ADLs samples and 156 FAs samples, and 7678 testing samples, which consist of 7600 ADLs samples and 78 FAs samples, are used. Thus, for

Table 6
Weights of the four activation functions of ESAEs-OCCCH in the ten trials.

Weight	1	2	3	4	5	6	7	8	9	10
Sigmoid	0.4088	0.4063	0.2868	0.0714	0.2765	0.2243	0.3234	0.1158	0.3514	0.3333
Relu	0.0231	0.0937	0.1029	0.1905	0.0284	0	0	0.1983	0.3514	0
Softplus	0.3526	0.2500	0.2500	0.4683	0.3121	0.3645	0.4431	0.3223	0.0810	0.4804
Gaussian	0.2155	0.2500	0.3603	0.2698	0.3830	0.4112	0.2335	0.3636	0.2162	0.1863

Table 7
Fall detection results of ESAEs-OCCCH and twelve SAEs-OCCCHs.

		Specificity	Sensitivity	Gmean	Average training time (s)	Average testing time (s)
Sigmoid	SAE1	99.37% ± 0.0022	92.73% ± 0.0036	95.99% ± 0.0020	151.87	0.08
	SAE2	99.50% ± 0.0018	91.55% ± 0.0056	95.44% ± 0.0029	90.49	0.02
	SAE3	99.03% ± 0.0020	93.84% ± 0.0039	96.40% ± 0.0022	153.61	0.03
Relu	SAE1	99.08% ± 0.0018	91.50% ± 0.0040	95.21% ± 0.0022	169.75	0.09
	SAE2	99.37% ± 0.0022	87.84% ± 0.0160	93.42% ± 0.0080	109.61	0.03
	SAE3	97.27% ± 0.0049	91.42% ± 0.0123	94.30% ± 0.0069	168.40	0.05
Softplus	SAE1	99.16% ± 0	92.58% ± 0.0051	95.81% ± 0.0027	160.20	0.10
	SAE2	98.36% ± 0.0013	92.88% ± 0.0046	95.58% ± 0.0025	106.40	0.03
	SAE3	97.90% ± 0.0020	95.58% ± 0.0070	96.73% ± 0.0037	171.44	0.05
Gaussian	SAE1	98.87% ± 0.0022	92.42% ± 0.0040	95.61% ± 0.0025	151.87	0.08
	SAE2	97.19% ± 0.0040	91.04% ± 0.0043	94.06% ± 0.0033	90.49	0.02
	SAE3	85.33% ± 0.0087	94.82% ± 0.0058	89.95% ± 0.0060	153.61	0.03
Ensemble		98.92% ± 0.0018	96.09% ± 0.0026	97.45% ± 0.0011	1858.27	0.66

The format of the specificity, sensitivity and gmean is mean (%) ± standard deviation.

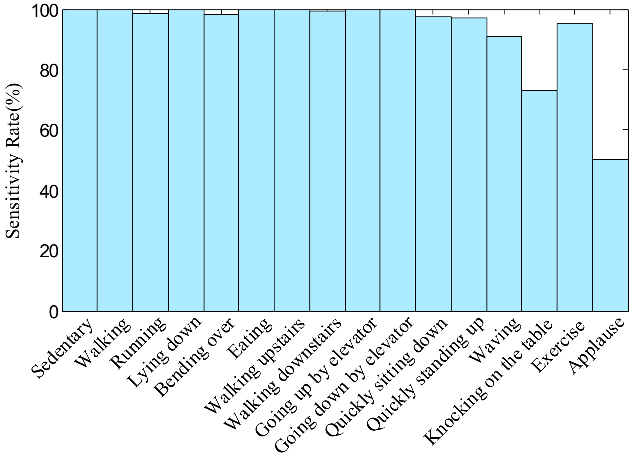

Fig. 8. Average sensitivities of the ADLs in experiment I.

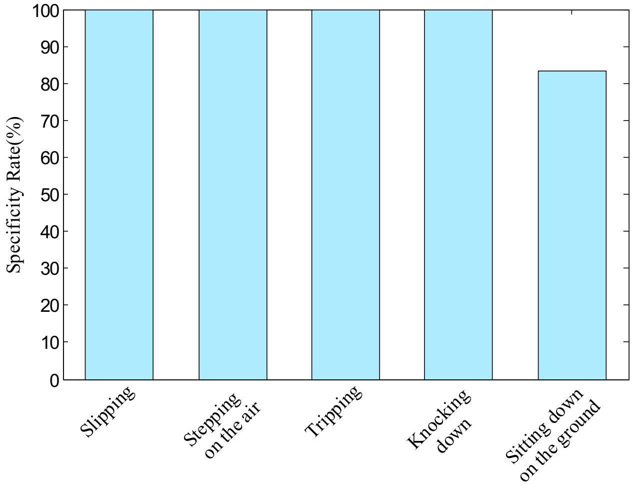

Fig. 9. Average specificities of the FAs in experiment I.

OCCCH and OCSVM, there are 19,200 training samples and 7678 testing samples. All comparisons are repeated ten times. The main parameters of the four methods with statistical features are listed in Table 9. The values of these parameters are obtained via many trials.

The average evaluation indices of the proposed method and the four comparison methods with 30 statistical features over ten trials are shown in Fig. 10. The specificities of the five methods

Table 8
Thirty statistical features for fall detection.

Domain	Statistical feature	Number
Time	Mean (X, Y, Z)	3
	Total mean	1
	Variance (X, Y, Z)	3
	Skewness (X, Y, Z)	3
	Kurtosis (X, Y, Z)	3
	Range (X, Y, Z)	3
	Total range	1
	Mean crossing rate (X, Y, Z)	3
	Absolute area (X, Y, Z)	3
	Total absolute area	1
Frequency	Mean (X, Y, Z)	3
	Standard Deviation (X, Y, Z)	3

Table 9
Main parameters of the four comparison methods.

Classifier	Description	Value
OCCCH with 30 features	Kernel function parameter	RBF kernel
	Kernel parameters σ	2
	Reduction factor μ	1
OCSVM with 30 features	Kernel function parameter	RBF kernel
	Kernel parameters σ	2
	Regularization parameter ν	0.1
SVM with 30 features	Kernel function parameter	RBF kernel
	Kernel parameters σ	2
KNN with 30 features	Number of neighbors k	7

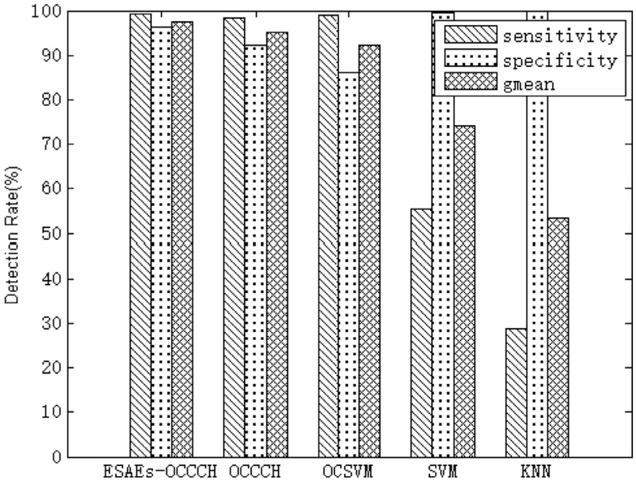

Fig. 10. Average evaluation indices of five methods based on ten trials.

(ESAEs-OCCCH, OCCCH, OCSVM SVM, and KNN) are 96.25%, 92.12%, 86.05%, 99.49%, 99.97%, respectively; the sensitivities are 99.13%, 98.42%, 99.03%, 55.46%, and 28.75%, respectively; and the gmeans are 97.45%, 95.22%, 92.31%, 74.12%, and 53.46%, respectively. The specificity, sensitivity, and gmean of the proposed method are 4.13%, 0.71%, and 2.23% higher compared to OCCCH with 30 features. Thus, the ESAEs outperform the artificial statistical features in unsupervised feature extraction. The comparison of OCCCH and OCSVM with 30 features demonstrates that although the specificity of OCSVM is slightly higher than that of OCCCH, its specificity and gmean are 6.07% and 2.91% lower than those of OCCCH respectively. Hence, OCCCH outperforms OCSVM in pattern recognition. Although the specificities of SVM and KNN with 30 statistical features exceed 99%, their sensitivities are less than 60% and their gmeans are less than 75% because of the data imbalance between ADLs and FAs. The comparisons in this section demonstrate the superior performance of ESAEs-OCCCH.

4.3. Implementability analysis

The implementability of the proposed method in terms of efficiency is discussed in this section. In the ten trials of Section 4.1, the average running time of the proposed method has been analyzed and compared with those of the twelve SAEs-OCCCHs, as presented in the last two columns of Table 7 (Core i5 with 8-GB random access memory). The average training time for 21,200 training samples of the proposed method is 1858.27 s, which is much longer than the average training times of the twelve SAEs-OCCCHs. The average testing time for 7834 testing samples of the proposed method is 0.66 s, which is much longer than those of the twelve SAEs-OCCCHs, but it is acceptable. Although training the model is time-consuming, the training and updating of the model will be completed in the background server system; only the testing will be executed on the smart watch. The results demonstrate the implementability of the proposed method in terms of efficiency.

To further evaluate the efficiency of the proposed method, the average running times of the proposed method and four compared classifiers with 30 statistical features over ten trials are compared and listed in Table 10. The average training time for 21,200 training samples of the proposed method is 1810.20 s, which is approximate to 1858.27 s in the first comparison, much longer than those of OCCCH, SVM, and KNN with statistical features. The average testing time for 7678 testing samples of the proposed method is 0.54 s, which is approximate to 0.66 s in the first comparison. The average training time and the average testing time of OCCCH with statistical features are 147.78 s and 0.15 s, respectively. These times are much shorter than the average training time and the average testing time of OCSVM with statistical features; hence, OCCCH performs more efficiently than OCSVM. Table 10 and Fig. 10 show that although the average testing times of SVM and KNN with statistical features are shorter than that of ESAEs-OCCCH and although the specificities of SVM and KNN exceed 99%, the sensitivities and gmeans are less than 60% and 75%, respectively. In summary, the comparisons demonstrate that the proposed method outperforms the other four methods in terms of comprehensive performance. Regarding the memory of the smart watch, ten minutes of data collection consumes 3 MegaByte memory and the physical memory of the watch is 4 GigaByte, which is sufficient for saving the data for one day. The results of the above analyses demonstrate the implementability of the proposed method.

In addition, it should be noted that because the binary-class methods such as SVM and KNN are used as comparison methods, two-thirds samples of the FAs are used for training and one-third are used for testing in Section 4.2. However, all FAs samples are used for testing in Section 4.1. The average training time and the average testing time of ESAEs-OCCCH in Tables 7 and 10 are slightly different, which verified the stability of the proposed method.

4.4. Extended experiment II and analysis

In experiment I, all ADLs and FAs are performed by the same six volunteers and the activities are performed in according to the activity classifications; thus, the training and testing samples may have commonalities. To exclude the influence of the experimenters and evaluate the expandability of the proposed method, extended experiment II is conducted, as discussed in Section 3.4. In this experiment, the testing samples consist of 2000 ADLs samples and 55 FAs samples. The ESAEs-OCCCH model, which was constructed in Section 4.1, was applied to the sample sets. The specificity, sensitivity and gmean of the proposed method reach 96.36% (53/55), 99.30% (1986/2000), and 97.82%, respectively. The results of extended experiment II further demonstrate the satisfactory performance of the ESAEs-OCCCH method.

5. Conclusions

Aiming at overcoming the limitations of currently available fall detection solutions for the elderly based on wrist-worn devices, which have high acceptance but perform poorly in terms of performance due to the complicated and frequent random movements of the hand and wrist, this paper proposes a novel fall detection method, namely, ESAEs-OCCCH. This method is based on accelerometer data from a wrist-worn smart watch. ESAEs are adopted for unsupervised feature extraction, and OCCCH is used for pattern recognition. To improve the performance and stability of fall detection, twelve SAEs-OCCCHs that differ in terms of SAEs architectures and activation functions are designed, and the majority voting strategy and adaptive weight adjustment strategy are used as ensemble strategies. Considering the behavioral characteristics of the elderly, the uncertainty of ADLs and FAs, and the influence of the intense activities of the hand on the accelerometer signal, thirteen FAs and sixteen ADLs, including intense activities of the hands, are designed and performed in two experiments by young volunteers of various genders, ages, heights and weights. The experimental results demonstrate that ESAEs-OCCCH is more effective and stable than the twelve SAEs-OCCCHs, the specificity, sensitivity, and gmean of the proposed method reach 98.92%, 96.09%, and 97.45% respectively, and the proposed method outperforms four methods (OCCCH, OCSVM, SVM, and KNN with statistical features) in fall detection. The results of extended experiment II further demonstrate the satisfactory performance of the proposed method, which realizes 96.36% specificity, 99.30% sensitivity, and 97.82 gmean. The experimental results demonstrate the performance and stability of the proposed method.

Table 10
Average times of five methods over ten trials.

	ESAEs-OCCCH	OCCCH	OCSVM	SVM	KNN
average training time (s)	1810.20	147.78	2355.47	826.70	39.64
average testing time (s)	0.54	0.15	0.20	0.08	0.05

Acknowledgements

This work is supported by the National Natural Science Foundation of China (Grant No. 51605151), the Innovation on working methodology of Chinese Ministry of Science & Technology (Grant No. 2016IM030300), and the Independent Research Work of the State Key Laboratory of Advanced Design and Manufacture for Vehicle Bodies (Grant No. 71675001). Thanks to all volunteers who participated in the experiments. The readers can contact us via email and ask for the datasets for non-commercial purposes.

References

[1] C.Y. Hsieh, K.C. Liu, C.N. Huang, W.C. Chu, C.T. Chan, Novel hierarchical fall detection algorithm using a multiphase fall model, Sensors 17 (2) (2017) 307.
[2] N. Noury, A smart sensor for the remote follow up of activity and fall detection of the elderly, in: Proc. of the IEEE Special Topic Conference on Microtechnologies in Medicine and Biology May, 2002, pp. 314–317.
[3] G. Baldewijns, G. Debard, G. Mertes, T. Croonenborghs, B. Vanrumste, Improving the accuracy of existing camera based fall detection algorithms through late fusion, Int. Conf. IEEE Eng. Med. Biol. Soc. (2017) 2667–2671.
[4] C.S. Lin, H.C. Hsu, Y.L. Lay, C.C. Chiu, C.S. Chao, Wearable device for real-time monitoring of human falls, Measurement 40 (9) (2007) 831–840.
[5] P.V. Er, K.K. Tan, Non-intrusive fall detection monitoring for the elderly based on fuzzy logic, Measurement 124 (2018) 91–102.
[6] A.K. Bourke, G.M. Lyons, A threshold-based fall-detection algorithm using a bi-axial gyroscope sensor, Med. Eng. Phys. 30 (1) (2008) 84–90.
[7] T.J. Shi, X.M. Sun, Z.H. Xia, L.Y. Chen, J.X. Liu, Fall detection algorithm based on triaxial accelerometer and magnetometer, Eng. Lett. 24 (2) (2016) 157–163.
[8] N. Pannurat, S. Thiemjarus, E. Nantajeewarawat, A hybrid temporal reasoning framework for fall monitoring, IEEE. SENS. J. 17 (6) (2017) 1749–1759.
[9] O. Aziz, M. Musngi, E.J. Park, A comparison of accuracy of fall detection algorithms (threshold-based vs. machine learning) using waist-mounted tri-axial accelerometer signals from a comprehensive set of falls and non-fall trials, Med. Biol. Eng. Comput. 55 (1) (2017) 45–55.
[10] M. Mubashir, L. Shao, L. Seed, A survey on fall detection: principles and approaches, Neurocomputing. 100 (2013) 144–152.
[11] W.C. Cheng, D.M. Jhan, Triaxial accelerometer-based fall detection method using a self-constructing cascade-adaboost-SVM classifier, IEEE J. Biomed. Health Inform. 17 (2) (2013) 411–419.
[12] P. Vallabh, R. Malekian, Fall detection monitoring systems: a comprehensive review, J. AMB. INTEL. HUM. COMP. 9 (6) (2018) 1809–1833.
[13] M.D. Prieto, G. Cirrincione, A.G. Espinosa, Bearing fault detection by a novel condition-monitoring scheme based on statistical-time features and neural networks, IEEE Trans. Industr. Electron. 60 (8) (2013) 3398–3407.
[14] L. Jing, M. Zhao, P. Li, X. Xu, A convolutional neural network based feature learning and fault diagnosis method for the condition monitoring of gearbox, Measurement 111 (2017) 1–10.
[15] A.N. Aicha, G. Englebienne, K.V. Schooten, M. Pijnappels, Deep learning to predict falls in older adults based on daily-life trunk accelerometry, Sensors 18 (5) (2018).
[16] S.G. Yoo, D. Oh, An artificial neural network-based fall detection, Int. J. Eng. Bus. Manag. 10 (2018).
[17] M. Kangas, A. Konttila, I. Winblad, Determination of simple thresholds for accelerometry-based parameters for fall detection, Int. Conf. IEEE Eng. Med. Biol. Soc. 1367 (2007).
[18] A.T. Özdemir, An analysis on sensor locations of the human body for wearable fall detection devices: principles and practice, Sensors 16 (8) (2016) 1161.
[19] M. Gjoreski, H. Gjoreski, M. Luštrek, M. Gams, How accurately can your wrist device recognize daily activities and detect falls, Sensors 16 (6) (2016) 800.
[20] Josef Stefan Institute. Ambient Intelligence Repository (AmI Repository). Available online (accessed on 15 May 2016): http://dis.ijs.si/ami-repository/.
[21] J. Yuan, K.K. Tan, T.H. Lee, C.H. Gerald, Power-efficient interrupt-driven algorithms for fall detection and classification of activities of daily living, IEEE Sens. J. 15 (3) (2015) 1377–1387.
[22] N. Pannurat, S. Thiemjarus, E. Nantajeewarawat, Automatic fall monitoring: a review, Sensors. 14 (7) (2014) 12900–12936.
[23] C.C. Zhou, C.L. Tu, Y. Gao, F.X. Wang, H.W. Gong, P. Lian, A low-power, wireless, wrist-worn device for long time heart rate monitoring and fall detection, IEEE Int. Conf. Orange Technol. IEEE (2014) 33–36.
[24] A.H. Ngu, P.T. Tseng, M. Paliwal, C. Carpenter, W. Stipe, Smartwatch-based IoT fall detection application, Open J. Int. Things. 4 (1) (2018) 87–98.
[25] T.D. Quadros, A.E. Lazzaretti, F.K. Schneider, A movement decomposition and machine learning-based fall detection system using wrist wearable device, IEEE Sens. J. 18 (12) (2018) 5082–5089.
[26] S.S. Khan, B. Taati, Detecting unseen falls from wearable devices using channel-wise ensemble of autoencoders, Expert. Syst. Appl. 87 (2017) 280–290.
[27] T. Zhang, J. Wang, L. Xu, P. Liu, Fall detection by wearable sensor and one-class SVM algorithm, Lect. Notes Contr. Inf. 345 (2006) 858–863.
[28] M. Zeng, Y. Yang, S.R. Luo, J.S. Chen, One-class classification based on the convex hull for bearing fault detection, Mech. Syst. Singal Process. 81 (2016) 274–293.
[29] V. Patraucean, A. Handa, R. Cipolla, Spatio-temporal video autoencoder with differentiable memory, Computer Science. 58 (11) (2015) 2415–2422.
[30] A.M. Karim, S. Güzel Mehmet, M.R. Tolun, H. Kaya, V. Çelebi Fatih, A new generalized deep learning framework combining sparse autoencoder and taguchi method for novel data classification and processing, Math. Probl. Eng. 2018 (3) (2018) 1–13.
[31] Z. Meng, X. Zhan, J. Li, Z. Pan, An enhancement denoising autoencoder for rolling bearing fault diagnosis, Measurement 130 (2018) 448–454.
[32] H. Shao, H. Jiang, Y. Lin, X. Li, A novel method for intelligent fault diagnosis of rolling bearings using ensemble deep auto-encoders, Mech. Syst. Singal Process. 102 (2018) 278–297.
[33] J.W. Wang, C. Sun, Z.B. Zhao, X.F. Chen, et al., Feature ensemble learning using stacked denoising autoencoders for induction motor fault diagnosis, Progn. Syst. Health Manag. Conf. (2017) 480–485.
[34] M. Sultan Zia, M. Hussain, M. Arfan Jaffar, A novel spontaneous facial expression recognition using dynamically weighted majority voting based ensemble classifier, Multimed. Tools Appl. 77 (19) (2018) 25537–25567.
[35] S.D. Bersch, D. Azzi, R. Khusainov, Sensor data acquisition and processing parameters for human activity classification, Sensors 14 (3) (2014) 4239–4270.
[36] S. Khojasteh, J.R. Villar, C. Chira, V.M. González, E.D.L. Cal, Improving fall detection using an on-wrist wearable accelerometer, Sensors 18 (5) (2018) 1350.
[37] P. Jatesiktat, A.T. Wei, An elderly fall detection using a wrist-worn accelerometer and barometer, Eng. Med. Biol. Soc. IEEE (2017) 125.